Naval Command,
Control and Ocean
Surveillance Center RDT&E Division
San Diego, CA
92152-5001

4

Technical Document 2720
November 1994

Multitone Matched-Field Processing in SWellEX-1

Philip W. Schey
Newell O. Booth

DISCLAIMER NOTICE

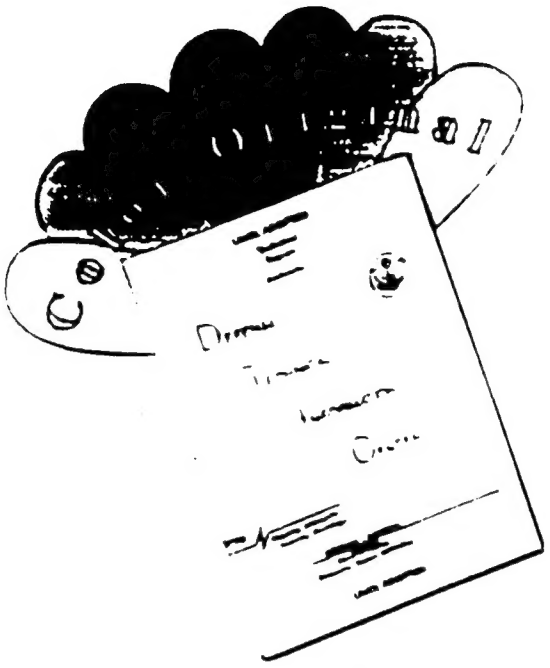

THIS DOCUMENT IS BEST QUALITY AVAILABLE. THE COPY FURNISHED TO DTIC CONTAINED A SIGNIFICANT NUMBER OF COLOR PAGES WHICH DO NOT REPRODUCE LEGIBLY ON BLACK AND WHITE MICROFICHE.

Technical Document 2720
November 1994

Multitone Matched-Field Processing in SWellEX-1

Philip W. Schey
Newell O. Booth

NAVAL OCEAN SYSTEMS CENTER
San Diego, California 92152–5000

K. E. EVANS, CAPT, USN
Commanding Officer

R. T. SHEARER
Technical Director

ADMINISTRATIVE INFORMATION

This work, conducted during FY 1994, was sponsored by the Office of Naval Research, Program Element 602314, Project RJ14K85, Task 541–SUB6.

Released by
Dr. C. D. Rees, Head
Acoustic Branch

Under authority of
Dr. J. H. Richter, Head
Ocean and Atmospheric
Sciences Division

SM

EXECUTIVE SUMMARY

OBJECTIVE

Determine the effectiveness of matched-field processing for source localization in a shallow-water environment.

APPROACH

Narrowband and multitone matched-field processing were performed on vertical line array data collected during the SWellEX-1 experiment, which was conducted off the coast of San Diego in August 1993.

RESULTS

While narrowband matched-field processing tended to produce ambiguous source localizations due to inexact propagation modeling, it was possible to accurately track the source by simultaneously processing the transmitted tones.

CONCLUSIONS

Multitone processing was effective in reducing the sensitivity to mismatch that can degrade the performance of narrowband matched-field processing. Multitone and broadband matched-field processing should be effective tools for source localization and tracking.

CONTENTS

FIGURES

INTRODUCTION

In August 1993, Shallow Water Evaluation Cell Experiment No. 1 (SWellEX-1), a study of propagation, matched-field processing (MFP) and ambient noise was conducted in a shallow-water area approximately 5 miles west of San Diego, CA. Figure 1 presents an overview of the site. Data were recorded on a 48-element, 88.125-m aperture, vertical line array suspended from the Scripps Institution of Oceanography's (SIO's) research vessel FLIP, which was moored at site "O" in figure 1. Acoustic element localization performed by SIO's Marine Physical Laboratory put the bottom element approximately 11 m off the bottom. Water depth at the array site was approximately 200 meters, so the array essentially spanned the bottom half of the water column. A source emitting tonals from 70 to 755 Hz was towed at depths from 20 to 80 m along an approximately range-independent path, G to I, and along a strongly range-dependent path, A to E. Bathymetric measurements and conductivity–temperature–depth (CTD) casts were made to support the analysis of the experimental data.

This report presents the results of matched-field processing in the SWellEX-1 experiment. The second section briefly discusses MFP itself and presents applications to data for the G to I track. The third section is a similar discussion for the A to E track. The last section summarizes the findings.

MATCHED-FIELD PROCESSING ALONG G TO I TRACK

One of the objectives of SWellEX-1 was to study the effectiveness of matched-field processing as a means of source localization in a shallow-water environment. Originally proposed by Bucker[1] in 1976, MFP has been an active area of research in underwater acoustics in recent years. Basically, MFP localizes a source by correlating the measured sound field at a hydrophone array with that predicted by a propagation model for a series of candidate source depths and ranges. A correlation peak indicates a high probability that the assumed source location corresponds to the true position. The correlation is defined as

$$C(f,r,z) = \frac{\sum_i \sum_j S_i^*(f,r,z) R_{ij}(f) S_j(f,r,z)}{\sum_i R_{ii}(f) \sum_i |S_i(f,r,z)|^2} \qquad (1)$$

Here, f is the source frequency, and r and z are, respectively, the range and depth of the assumed source location. The indices i and j refer to hydrophone numbers and the sums are over the elements of the array. $S_i(f,r,z)$ is the theoretical sound pressure at phone i produced by a source of frequency f located at range r and depth z. This was calculated using Collins' Finite Element Parabolic Equation program.[2] If $p_i(f)$ is the measured sound field at phone i and frequency f, then the covariance matrix, $R_{ij}(f)$, is calculated as $\langle p_i(f) p_j^*(f) \rangle$, where the brackets indicate a time average and the * indicates complex conjugate. A perfect match between the data and prediction would yield a correlation of unity.

---

[1]H. P. Bucker. 1976. "Use of Calculated Sound Fields and Matched-Field Detection to Locate Sound Sources in Shallow Water," J. Acoust. Soc. Am. 59, 368–373.

[2]M. D. Collins and E. K. Westwood. 1991. "A Higher-Order Energy-Conserving Parabolic Equation for Range-Dependent Ocean Depth, Sound Speed, and Density," J. Acoust. Soc. Am. 89, 1068–1075.

The G to I track was a nearly range-independent propagation path. Figure 2 illustrates the bathymetry and sound speed profile used in the calculations. The sound speed profile is from a CTD cast taken at site G at the same time of day as the data.

The data set analyzed covered the time period from 1615 to 1736 on 17 August 1993. The source moved outward from a range of 0.6 km to 8.2 km at a speed of approximately 3 knots. The tow depth varied somewhat but was generally between 80 and 85 m. The source track and the position of the receiving array in the water column are shown in figure 2.

Figure 3 is a single phone lofargram for the 0 to 250-Hz frequency band. The transmitted tones at 70, 95, 145, and 195 Hz are visible, along with numerous other spectral lines. The prominent line at 175 Hz is from FLIP. The broadband noise is due to a passing ship, which had closest point of approach (CPA) at approximately 1640. The 95-Hz tone is nearly obliterated by the noise at CPA. The signal-to-noise ratio was approximately 20 dB at the start of the track and dropped to 5 to 10 dB at the far end.

As presented above, MFP is a narrowband technique. That is, both the measured and predicted hydrophone sound fields are at one frequency. A problem encountered in narrowband MFP is that while there is high correlation at the correct source location, mismatch between the modeled and true propagation can result in correlation peaks of the same magnitude at other positions. These sidelobes make unambiguous source localization difficult. However, if the source emits several frequencies, Porter[3] has shown that simultaneous processing of the tones results in improved performance. Essentially, each frequency has a correlation peak at the true source location, but the positions of the sidelobes vary with frequency, so combining the frequencies will lower the sidelobe level relative to the true peak. While there are numerous ways in which the frequencies can be combined, a simple incoherent averaging scheme was found to be effective. For each assumed source location, the correlation in equation 1 is calculated separately for each of the M tones, and these correlations are then averaged to yield the final result:

$$C(r,z) = \frac{1}{M}\sum_{f} C(f,r,z) \qquad (2)$$

To illustrate, the top four frames in figure 4 are the matched-field range-depth surfaces for 70, 95, 145, and 195 Hz, respectively, at a time when the true range was 5.9 km and the depth was 85 m. The multiple correlation peaks in these plots make it difficult to say with much confidence where the source actually is. However, if these narrowband results are averaged as in equation 2 with $M = 4$, the bottom plot is obtained. The correlation maximum at a 5.9-km range and a 84-m depth agrees well with the true source location, and the localization is fairly unambiguous, in that the sidelobes are considerably weaker than the main peak.

To see how well the source could be tracked, the 81-minute data set was treated as a set of 1-minute segments, overlapped by 50 percent. For each of these segments, narrowband and frequency-averaged surfaces like those in figure 4 were generated, and for each surface, the range and depth at which the maximum correlation occurred was saved. Figure 5 summarizes the results. The left two frames plot the range and depth of the peak correlation vs time for each of

[3]M. B. Porter. 1994. "Source Tracking in the Hudson Canyon Experiment," J. Acoust. Soc. Am. 95, 2981.

frequency-averaged surfaces like those in figure 4 were generated, and for each surface, the range and depth at which the maximum correlation occurred was saved. Figure 5 summarizes the results. The left two frames plot the range and depth of the peak correlation vs time for each of the individual frequencies. There are a considerable number of false localizations where inexact modeling has resulted in a sidelobe having higher correlation than that at the true source location. The right two frames in figure 5 are similar plots for the frequency-averaged case. For comparison, the solid lines are the true range and depth vs time. Frequency-averaging has been effective in reducing the sidelobes and consequently the source depth and range tracks are accurately reproduced.

Rather than plot the matched-field output as a function of range and depth at a fixed time as in figure 4, we can fix the source depth and plot the output as a function of range and time. Figure 6 presents narrowband and frequency-averaged range–time plots for a source depth equal to the average tow depth, 82 m. The source track is clearest in the frequency-averaged plot, although the 145-Hz and 195-Hz narrowband results are also fairly unambiguous. As noted earlier, the 95-Hz tone was degraded by the broadband source. The 70-Hz tone has the highest correlation, but also has the highest sidelobes.

Two other data sets from the G to I track were analyzed in the same manner as above. Only the final results will be presented. From 1745 to 1910 on 17 August, the source was towed inward from I to G at a depth of approximately 80 m. Figure 7 is a plot of the range and depth of the correlation peak vs time for this data set. Finally, from 2205 to 2340 on 17 August, the source was again towed from I to G, but this time at a shallow depth of 20 m. Figure 8 summarizes the narrowband and frequency-averaged results. In these two data sets, as in figure 5, frequency-averaging has had the desired effect of suppressing the sidelobes so that reliable source tracking is possible.

MATCHED-FIELD PROCESSING ALONG A TO E TRACK

In contrast to the relatively benign G to I track, the A to E track was strongly range-dependent. Figure 9 illustrates the propagation environment. The sound speed profiles are from CTD casts taken at the indicated locations.

From 0956 to 1129 on 17 August, the source was towed outward at an average depth of 21 m from an initial range of 0.6 km to a final range of 9.2 km.

Figure 10 is a lofargram for this data set. The transmitted tones at 70, 95, 145, and 195 Hz are identified. The signal-to-noise ratio ranged from 15 to 20 dB at point A to approximately 5 dB at point E.

Figure 11 presents narrowband and frequency-averaged range–depth surfaces at a time when the range was 6.2 km and the depth was 21 m. The narrowband results are very ambiguous. The correlation peak for the frequency-averaged case is at a 6.2-km range and a 24-m depth, in agreement with the actual location, but the sidelobes are only slightly lower than the main peak. In general, frequency-averaging was not as successful in suppressing the sidelobes on this track as it was on the G to I track.

Figure 12, generated in the same manner as figure 5, plots the range and depth of the peak correlation vs time. The solid lines are the true range and depth tracks. Although the frequency-averaged plot shows some false localizations, the track is still fairly well defined. It is a marked improvement over the narrowband results, where there is hardly a hint of the source track.

Finally, figure 13 is a set of narrowband and frequency-averaged range–time plots for a source depth equal to the average tow depth, 21 m. The source track is better defined in the frequency-averaged plot than in any of the narrowband plots, although none of the tracks are as clear as their counterparts in figure 6 for the G to I track.

CONCLUSIONS

The idea of matched-field processing, localizing a source by comparing the measured and modeled propagation, is appealing. In practice, however, imprecise knowledge of environmental parameters can seriously degrade MFP's performance. Through analysis of data collected on the SWellEX-1 experiment, it was found that frequency-averaging is an effective means for reducing the sensitivity to modeling uncertainty, and makes unambiguous source tracking possible. While the scenario studied here, four widely spaced tones, is unlikely to occur in practice, the results indicate that MFP would be effective for true broadband sources.

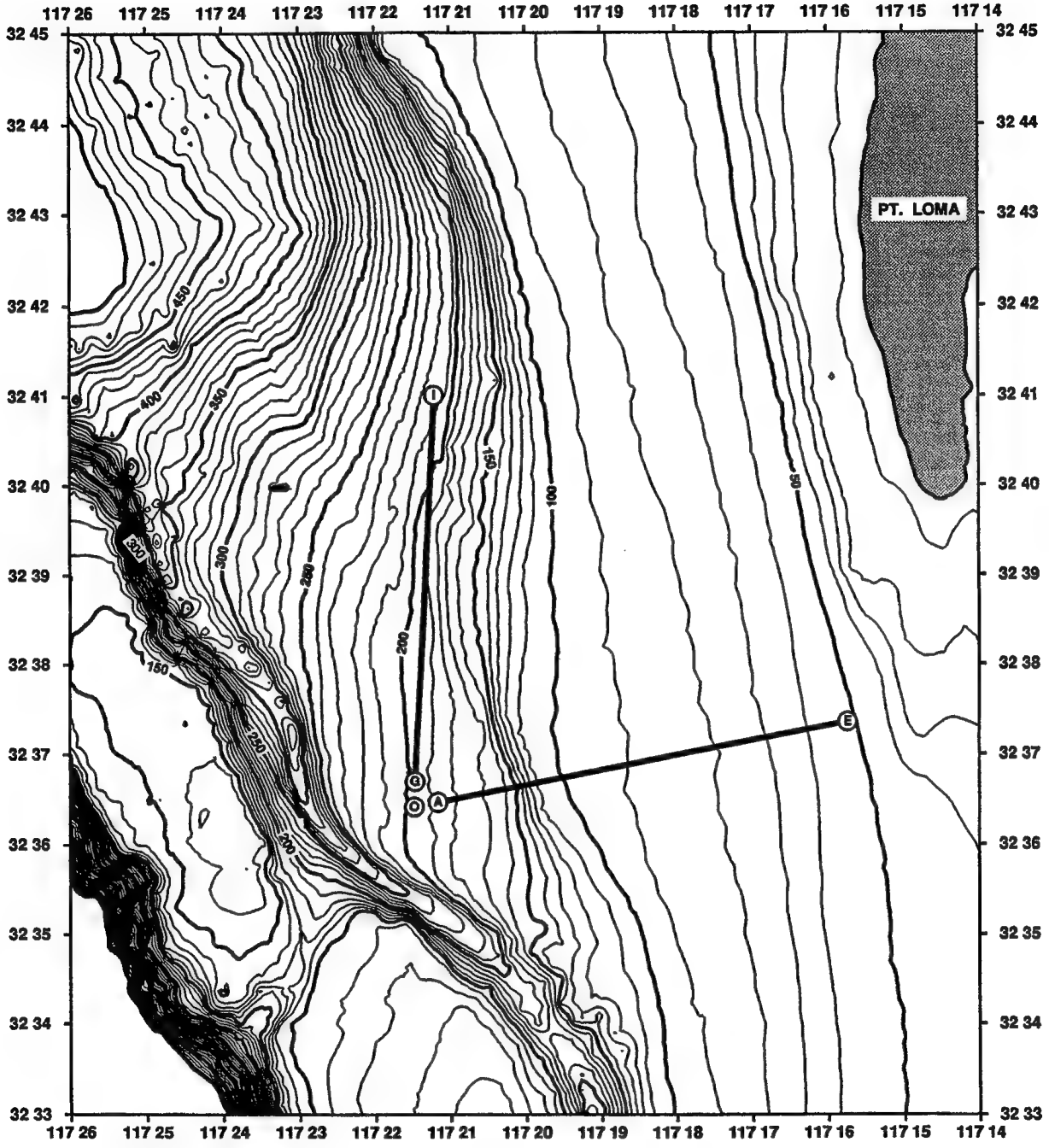

Figure 1. SWellEX-1 test area, August 1993.

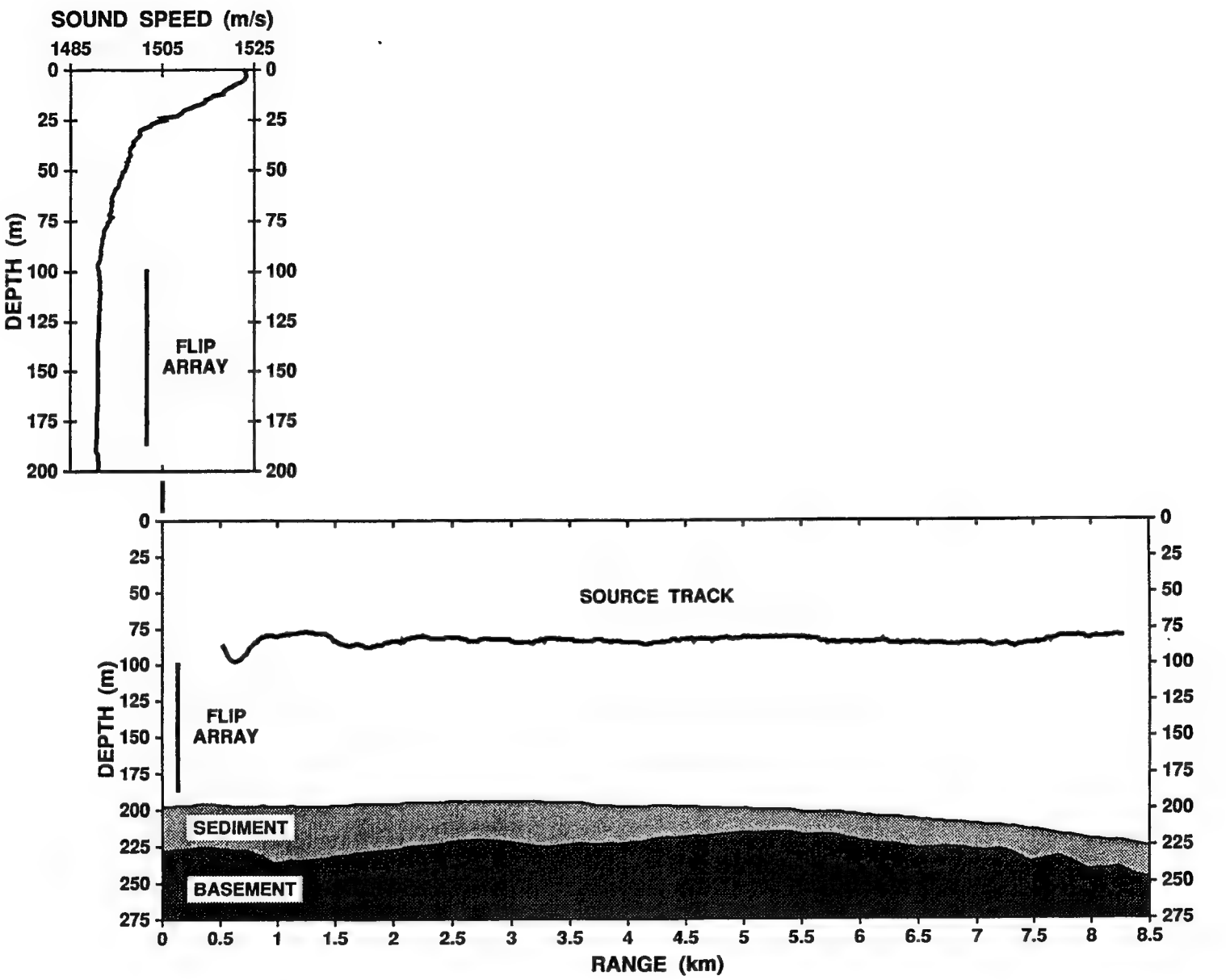

Figure 2. Track G to I—bathymetry, sediment thickness, and sound speed profile.

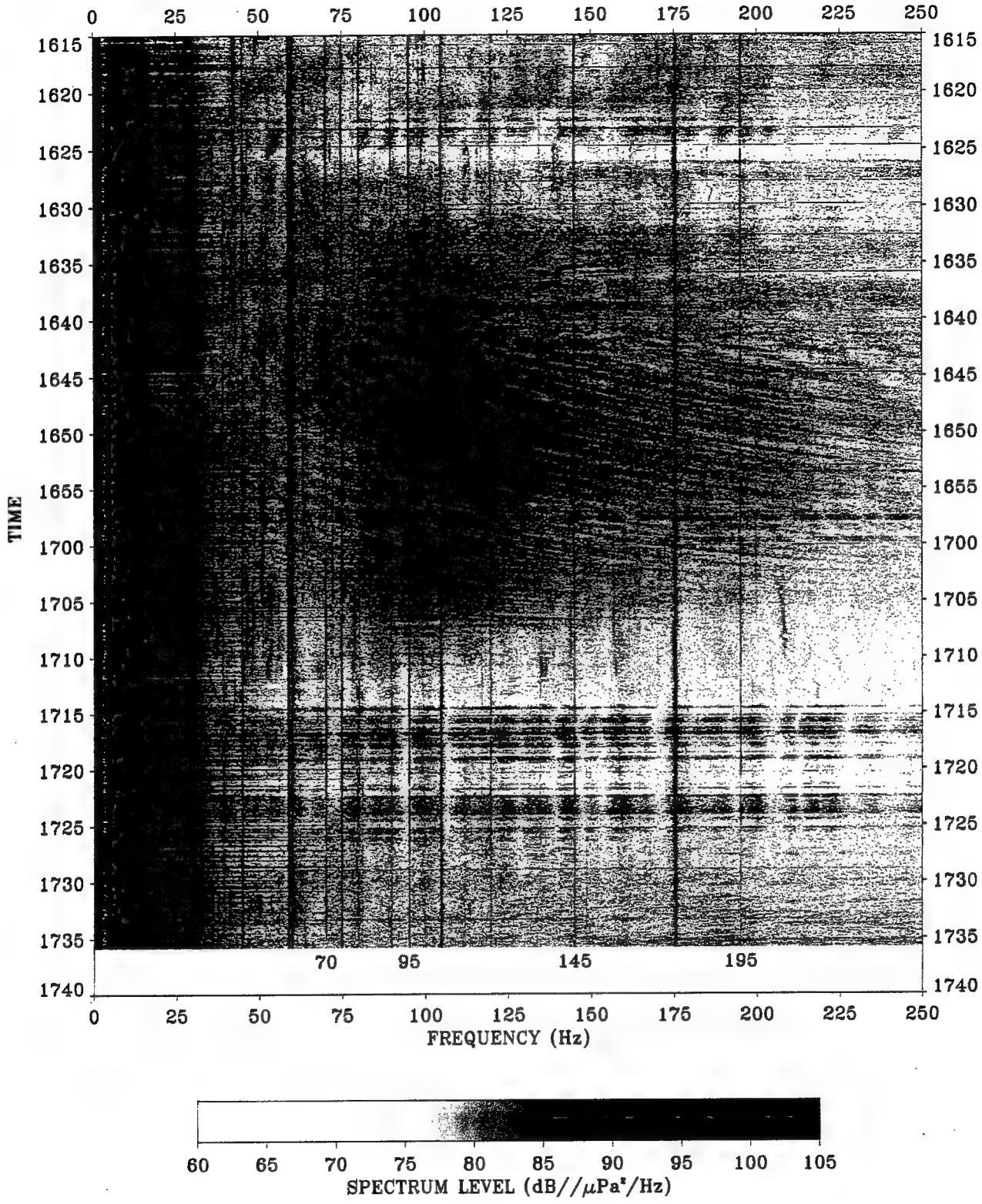

Figure 3. Track G to I, lofargram for Channel 24.

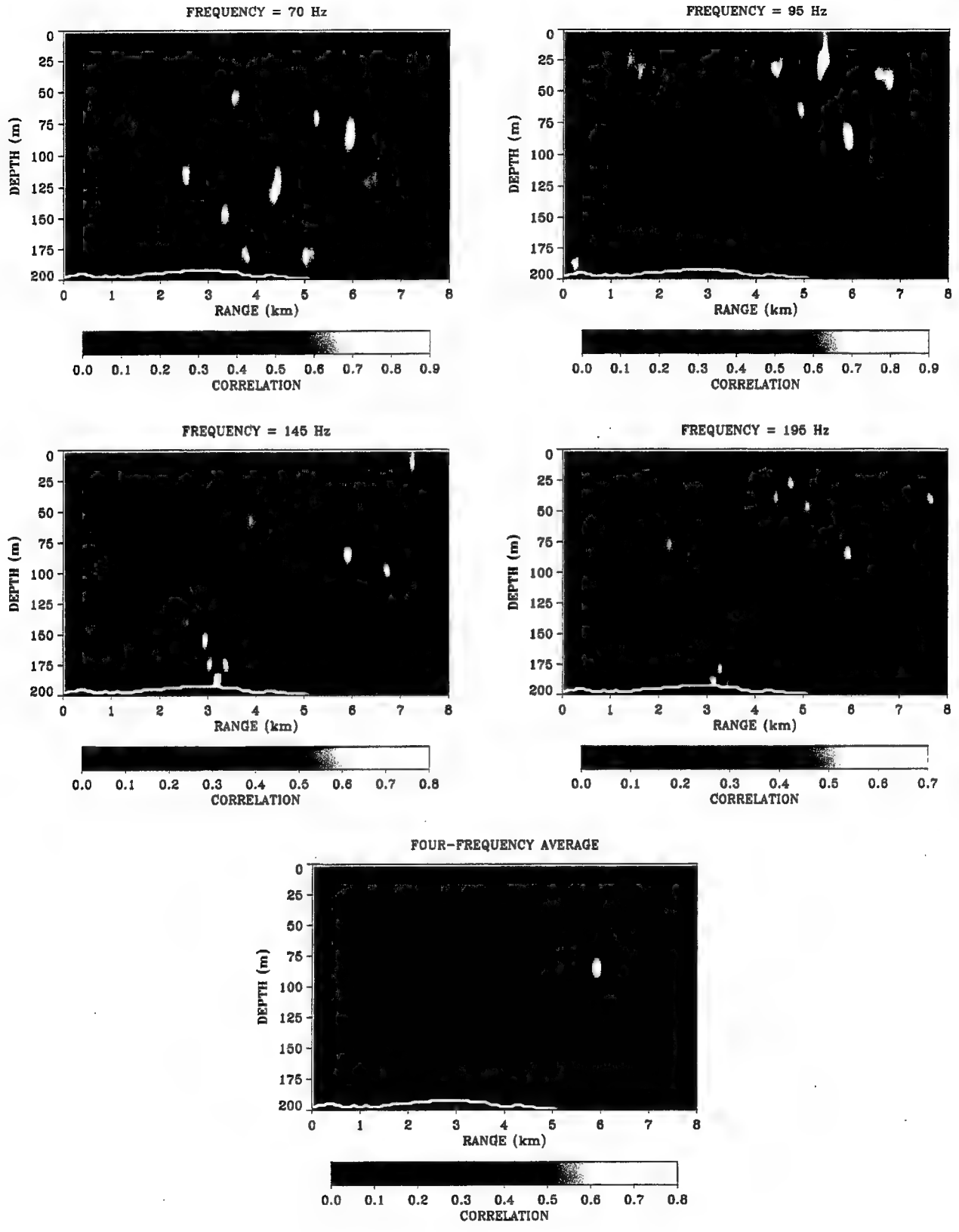

Figure 4. Track G to I, 1710 to 1711, true range = 5.9 km, true depth = 85 m.

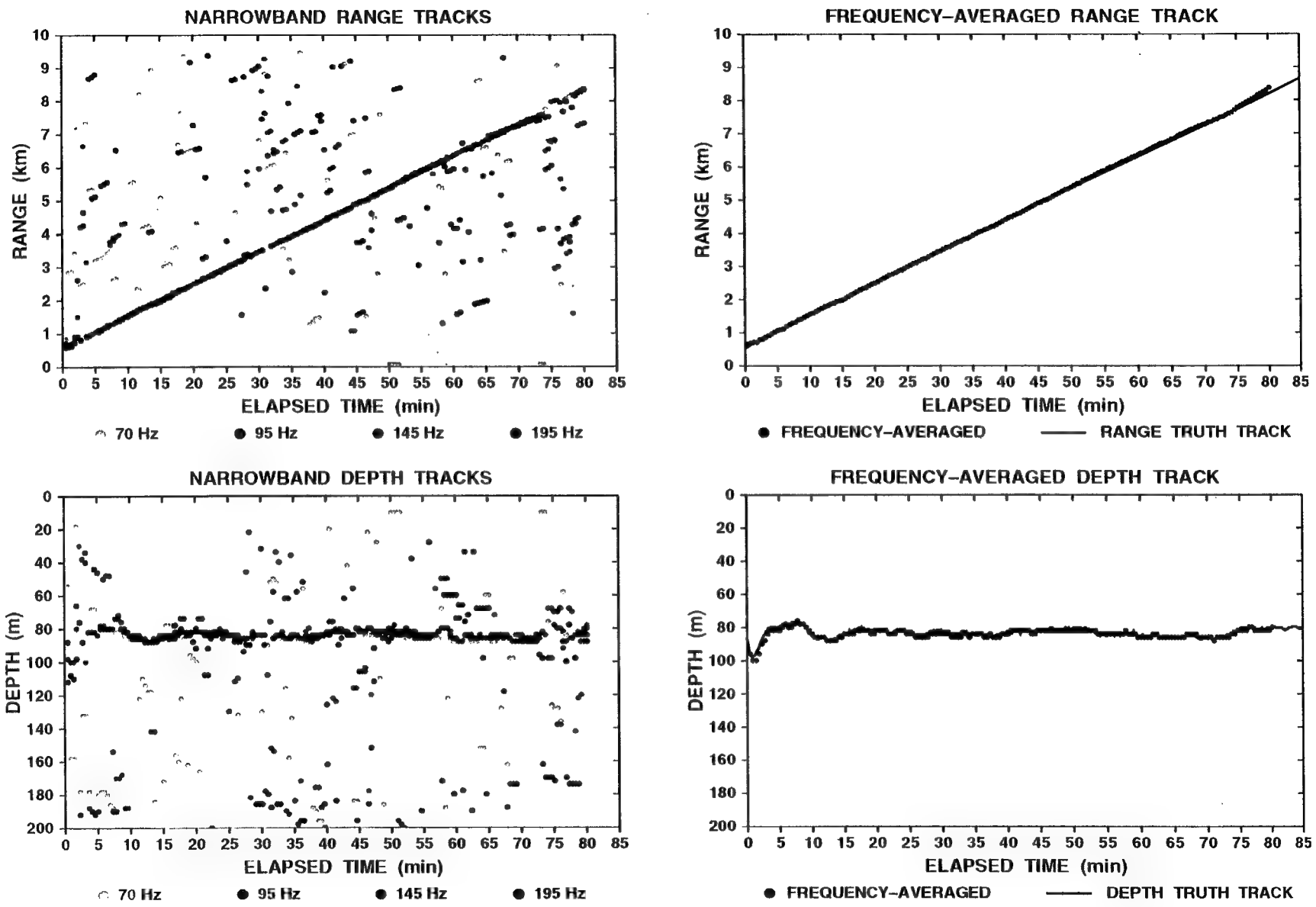

Figure 5. Track G to I, 1615 to 1740, source range and depth from MFP.

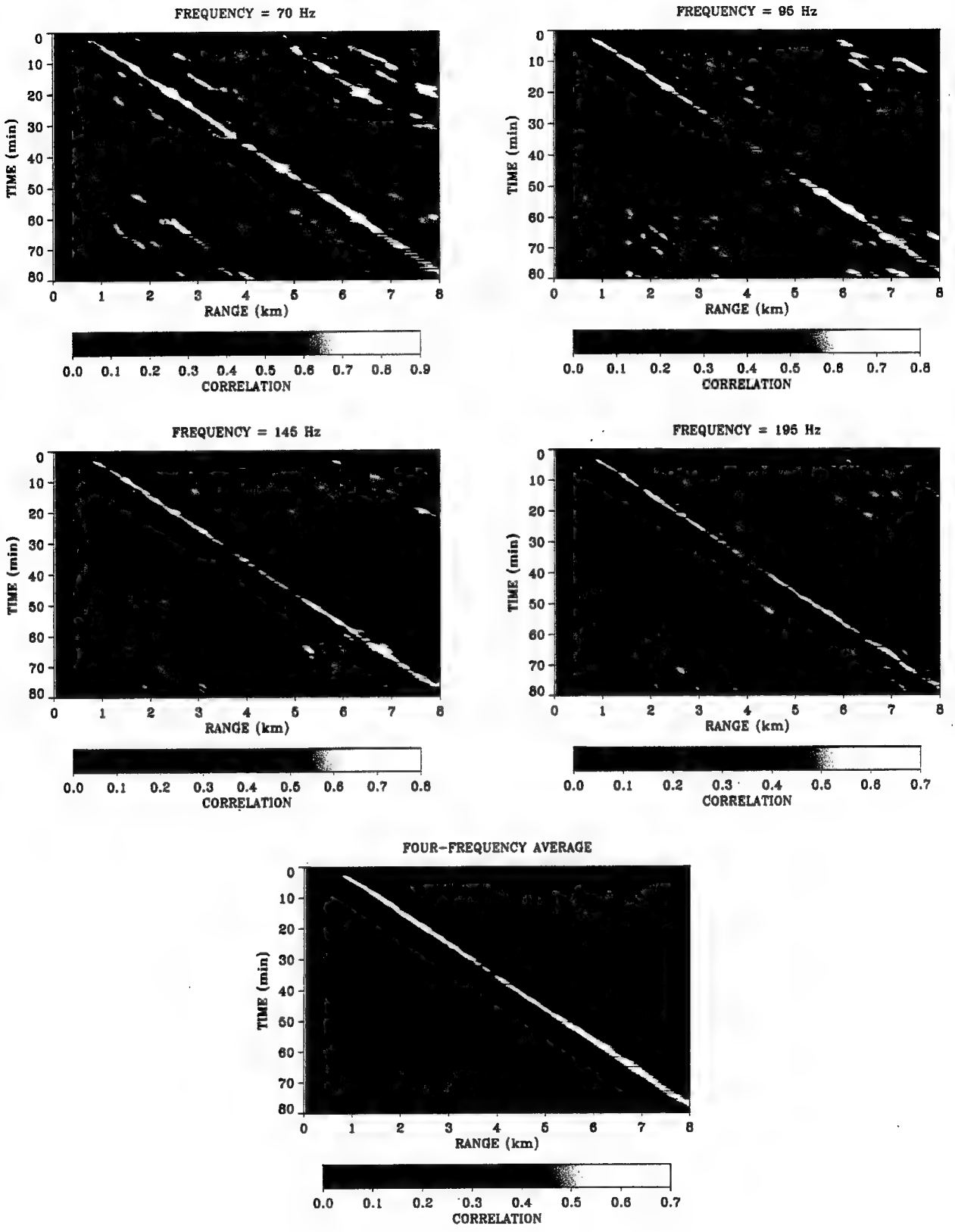

Figure 6. Track G to I, 1615 to 1735, source depth = 82 m.

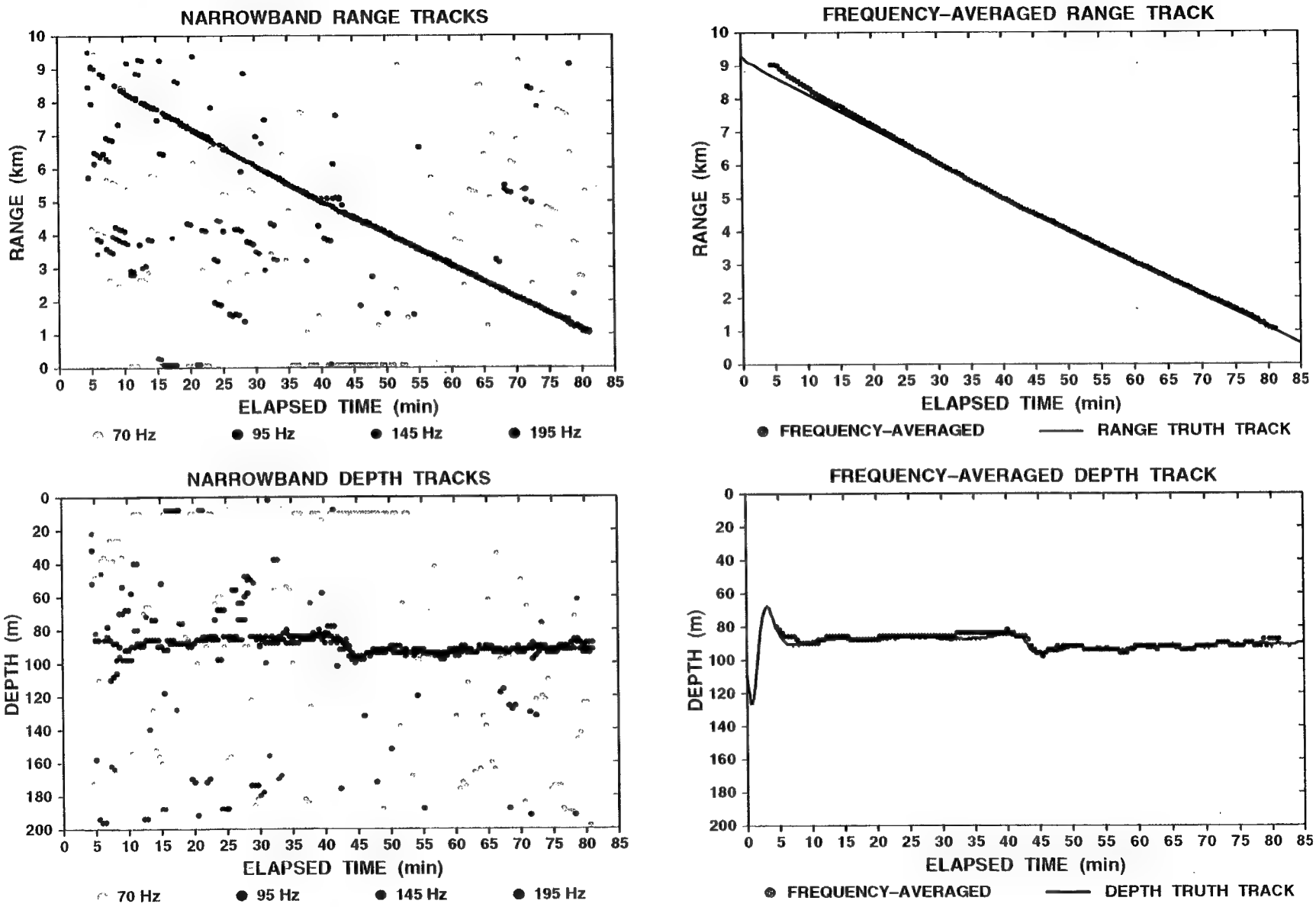

Figure 7. Track I to G, 1745 to 1910, source range and depth from MFP.

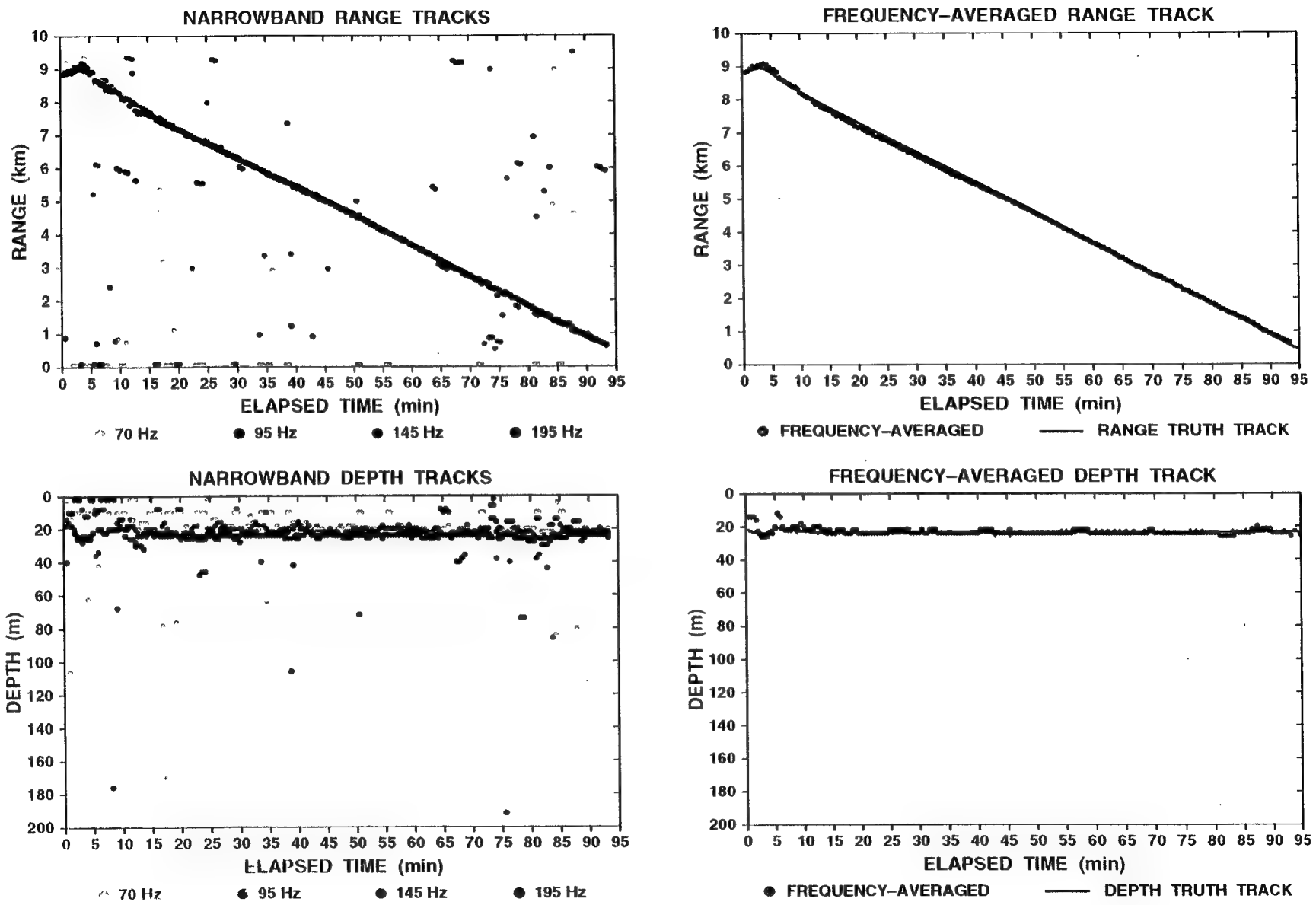

Figure 8. Track I to G, 2205 to 2340, source range and depth from MFP.

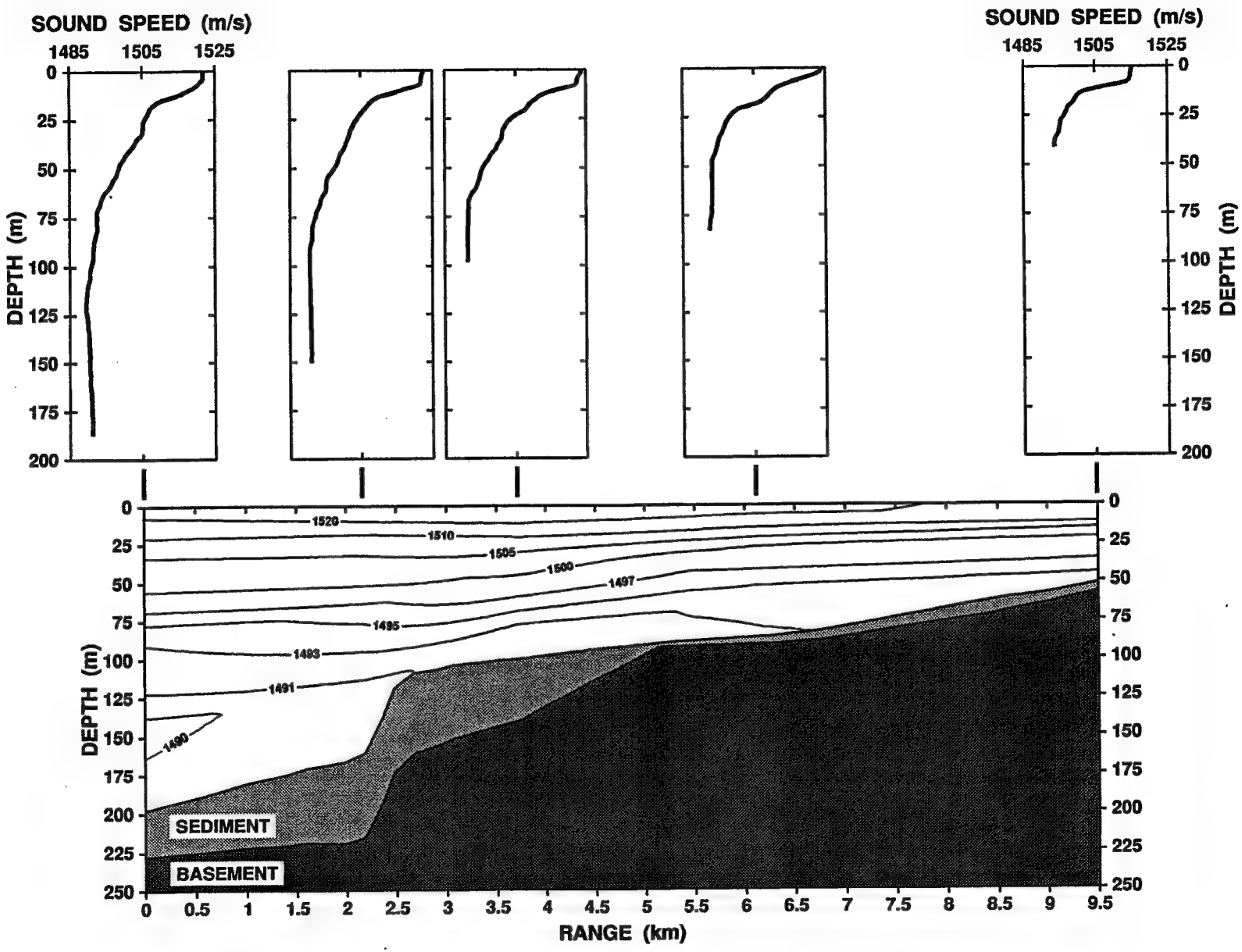

Figure 9. Track A to E—bathymetry, sediment thickness, and sound speed profiles.

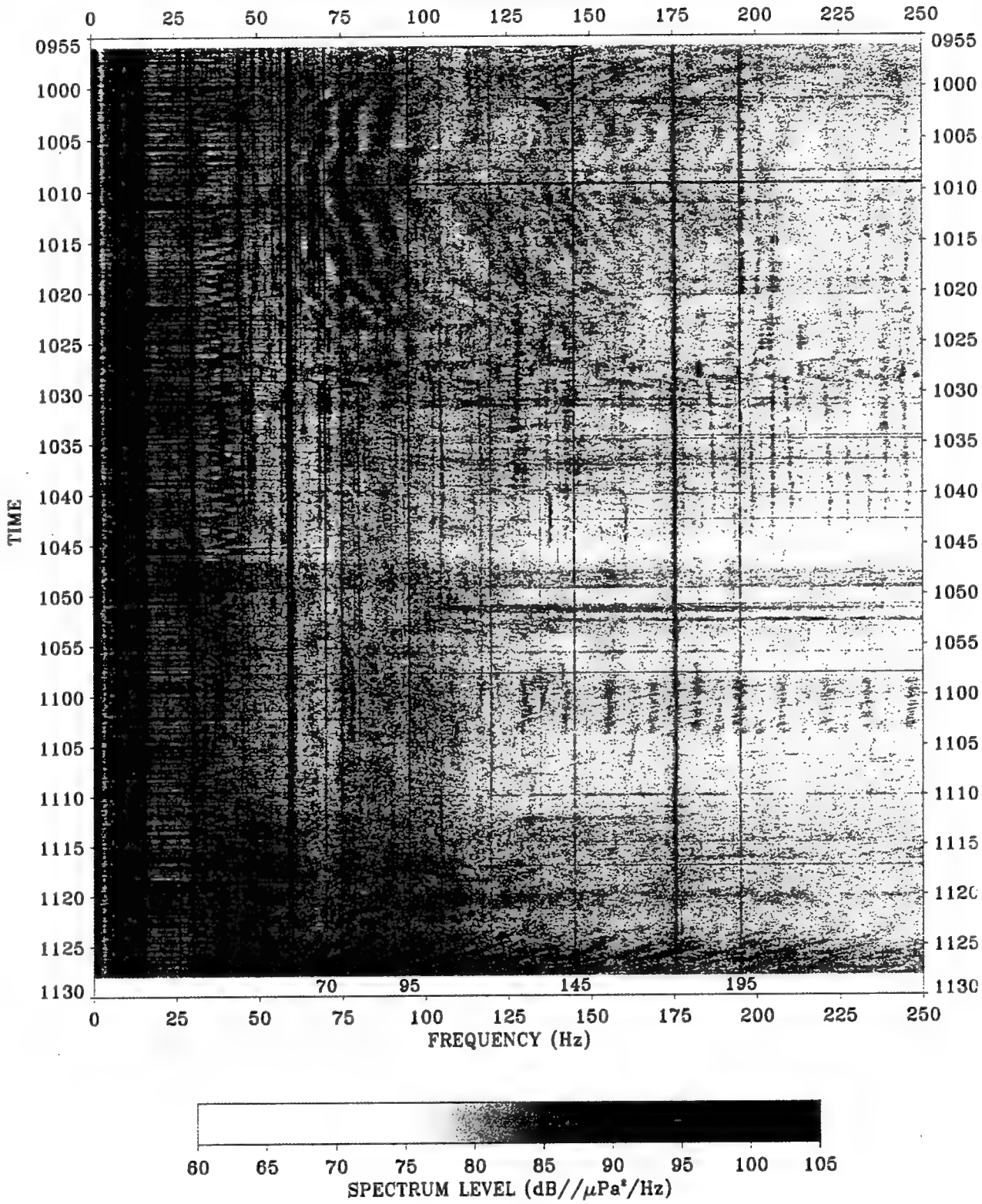

Figure 10. Track A to E, lofargram for Channel 24.

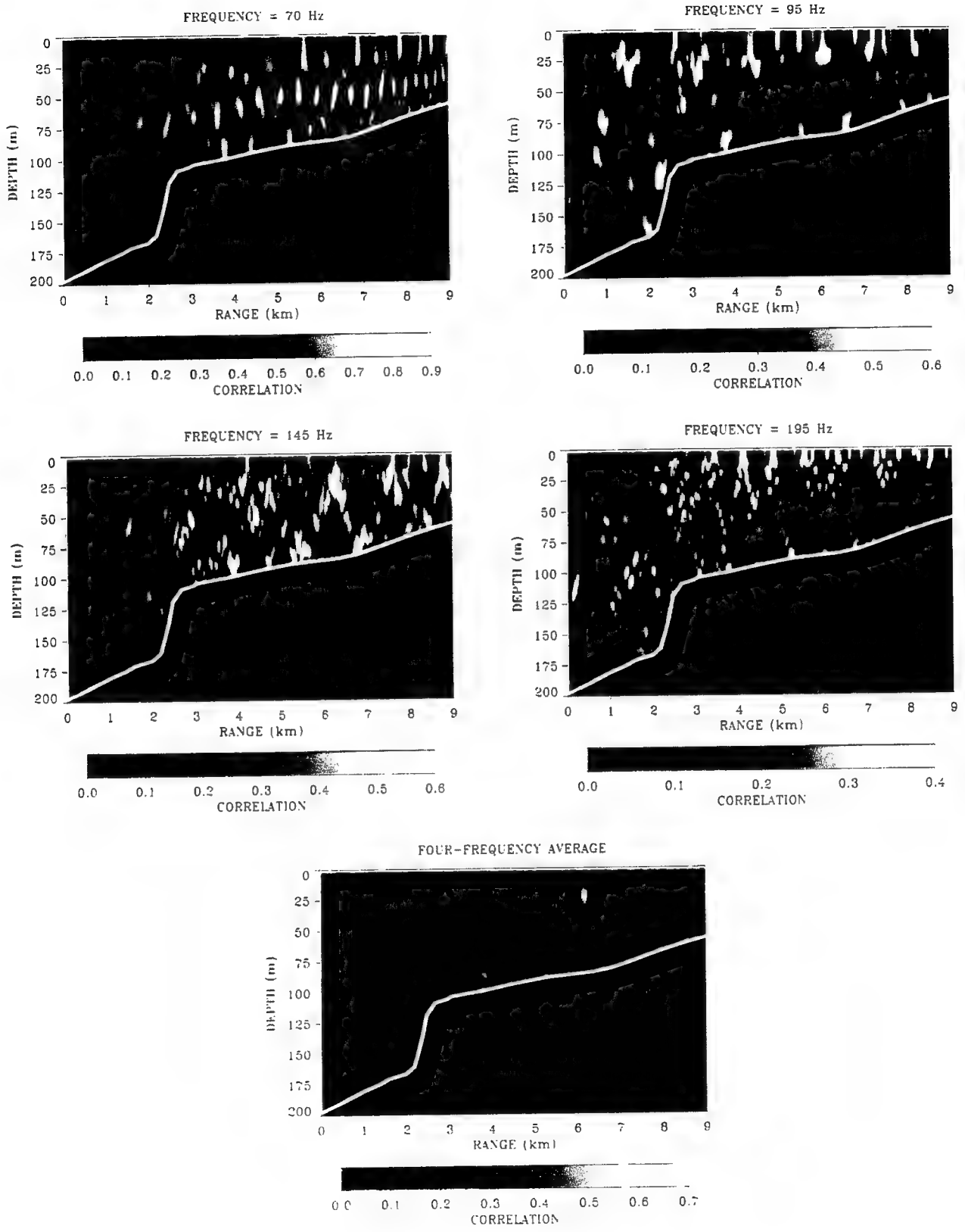

Figure 11. Track A to E, 1056 to 1057, true range = 6.2 km, true depth = 21 m.

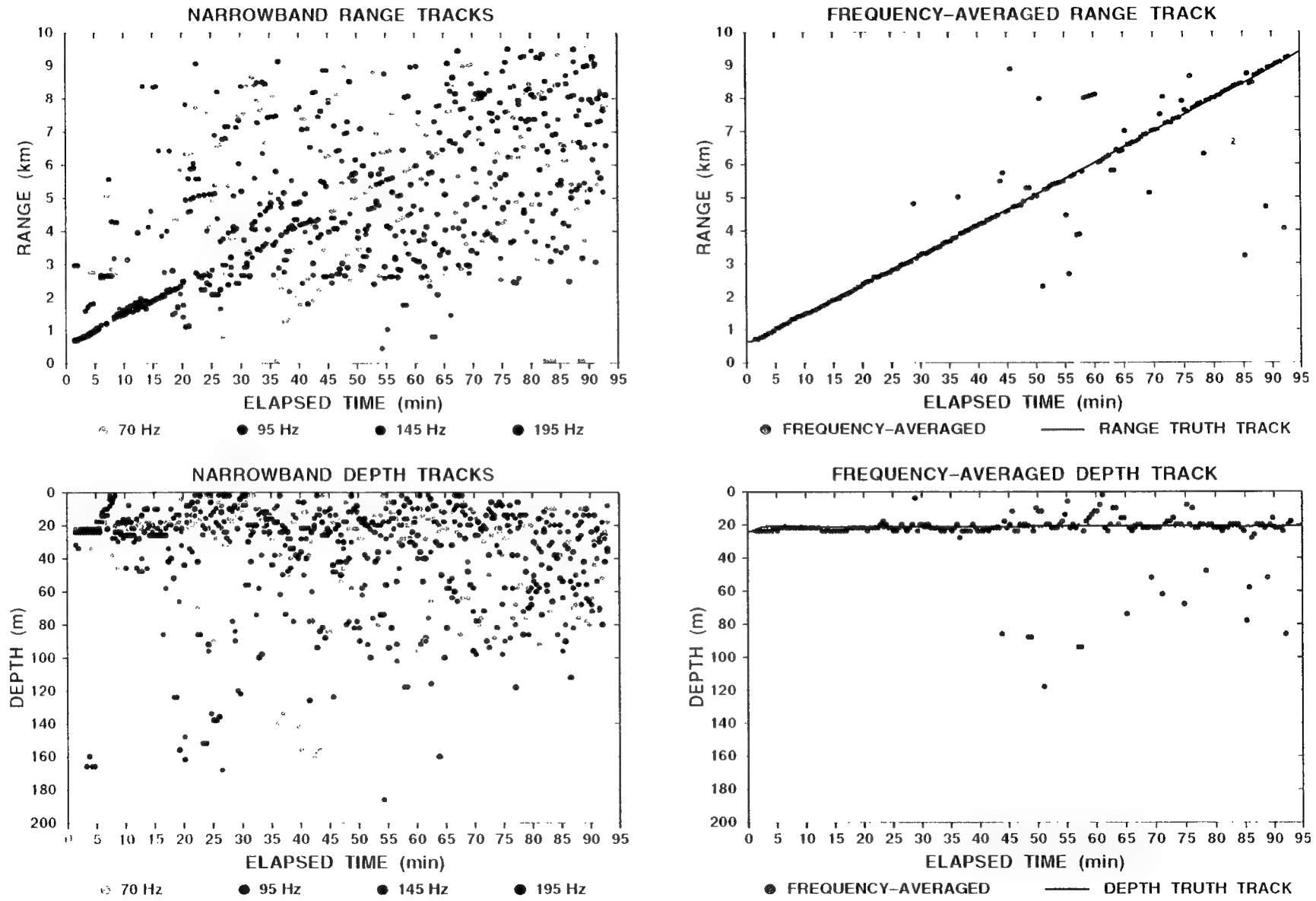

Figure 12. Track A to E, 0955 to 1130, source range and depth from MFP.

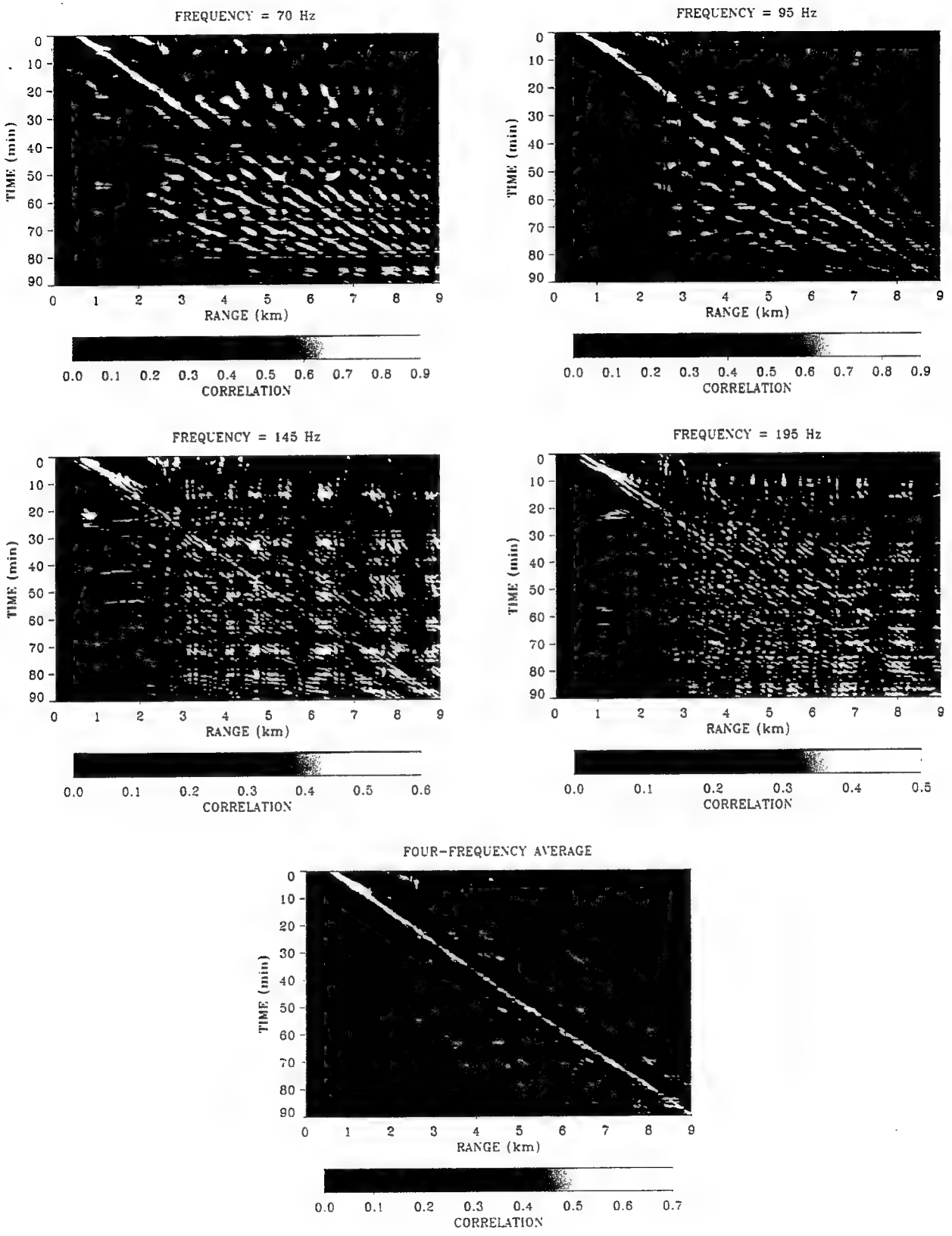

Figure 13. Track A to E, 0956 to 1126. source depth = 21 m.

REPORT DOCUMENTATION PAGE

Form Approved
OMB No. 0704-0188

1. AGENCY USE ONLY *(Leave blank)*	2. REPORT DATE	3. REPORT TYPE AND DATES COVERED
	November 1994	Interim: Oct 1993 – Oct 1994

4. TITLE AND SUBTITLE

MULTITONE MATCHED-FIELD PROCESSING IN SWellEX-1

5. FUNDING NUMBERS

PE: 0602314N
DN307363
WU: 541–SUB6
Project: RJ14K85

6. AUTHOR(S)

Philip W. Schey and Newell O. Booth

7. PERFORMING ORGANIZATION NAME(S) AND ADDRESS(ES)

Naval Command, Control and Ocean Surveillance Center (NCCOSC)
RDT&E Division
San Diego, California 92152–5000

8. PERFORMING ORGANIZATION REPORT NUMBER

TD 2720

9. SPONSORING/MONITORING AGENCY NAME(S) AND ADDRESS(ES)

Office of Naval Research
800 N. Quincy Street
Arlington, VA 22217

10. SPONSORING/MONITORING AGENCY REPORT NUMBER

11. SUPPLEMENTARY NOTES

12a. DISTRIBUTION/AVAILABILITY STATEMENT

Approved for public release; distribution is unlimited.

12b. DISTRIBUTION CODE

13. ABSTRACT *(Maximum 200 words)*

SWellEX-1 was a study of shallow-water propagation conducted near San Diego, CA, in August 1993. Data were recorded on an 88-meter aperture vertical line array while a source that emitted tonals from 70 Hz to 755 Hz was towed along range-independent and range-dependent tracks around the array site. One of the objectives was to study the effectiveness of matched-field processing as a means of source localization in a shallow-water environment. It was found that while narrowband matched-field processing tended to give ambiguous source localizations due to mismatch between the modeled and true propagation, it was possible to accurately track the source by simultaneously processing the transmitted tones.

14. SUBJECT TERMS

matched-field beamforming
matched-field processing
shallow-water acoustics

15. NUMBER OF PAGES

26

16. PRICE CODE

17. SECURITY CLASSIFICATION OF REPORT	18. SECURITY CLASSIFICATION OF THIS PAGE	19. SECURITY CLASSIFICATION OF ABSTRACT	20. LIMITATION OF ABSTRACT
UNCLASSIFIED	UNCLASSIFIED	UNCLASSIFIED	SAME AS REPORT

21a. NAME OF RESPONSIBLE INDIVIDUAL	21b. TELEPHONE *(include Area Code)*	21c. OFFICE SYMBOL
Philip W. Schey and Newell O. Booth	(619) 553–5613/2056	Code 541

INITIAL DISTRIBUTION

Code 0012	Patent Counsel	(1)
Code 0271	Archive/Stock	(6)
Code 0274	Library	(2)
Code 50	H. O. Porter	(1)
Code 54	J. H. Richter	(1)
Code 541	P. A. Baxley	(1)
Code 541	D. Rees	(1)
Code 541	F. J. Ryan	(1)
Code 541	P. W. Schey	(1)
Code 541	B. J. Sotirin	(1)
Code 541	N. O. Booth	(3)
Code 705	M. F. Morrison	(1)
Code 712	D. K. Barbour	(1)
Code 7801	B. Williams	(1)

Defense Technical Information Center
Alexandria, VA 22304–6145 (4)

NCCOSC Washington Liaison Office
Washington, DC 20363–5100

Center for Naval Analyses
Alexandria, VA 22302–0268

Navy Acquisition, Research and Development
Information Center (NARDIC)
Arlington, VA 22244–5114

GIDEP Operations Center
Corona, CA 91718–8000

Office of Naval Research
Arlington, VA 22217–5000 (3)

Naval Research Laboratory
Washington, DC 20375–5000 (2)

University of California, San Diego
Marine Physical Laboratory
San Diego, CA 92166–6049